STAR-Echo: A Novel Biomarker for Prognosis of MACE in Chronic Kidney Disease Patients Using Spatiotemporal Analysis and Transformer-Based Radiomics Models

Rohan Dhamdhere[1], Gourav Modanwal[1], Mohamed H. E. Makhlouf[2], Neda Shafiabadi Hassani[2], Satvika Bharadwaj[1], Pingfu Fu[3], Ioannis Milioglou[2], Mahboob Rahman[2,3], Sadeer Al-Kindi[2,3], and Anant Madabhushi[1,4(✉)]

[1] Wallace H. Coulter Department of Biomedical Engineering, Georgia Institute of Technology and Emory University, Atlanta, GA 30322, USA
anantm@emory.edu
[2] University Hospitals, Cleveland, USA
[3] Case Western Reserve University, Cleveland, OH, USA
[4] Atlanta Veterans Affairs Medical Center, Atlanta, GA, USA

Abstract. Chronic Kidney Disease (CKD) patients are at higher risk of Major Adverse Cardiovascular Events (MACE). Echocardiography evaluates left ventricle (LV) function and heart abnormalities. LV Wall (LVW) pathophysiology and systolic/diastolic dysfunction are linked to MACE outcomes (O^- and O^+) in CKD patients. However, traditional LV volume-based measurements like ejection-fraction offer limited predictive value as they rely only on end-phase frames. We hypothesize that analyzing LVW morphology over time, through spatiotemporal analysis, can predict MACE risk in CKD patients. However, accurately delineating and analyzing LVW at every frame is challenging due to noise, poor resolution, and the need for manual intervention. Our contribution includes (a) developing an automated pipeline for identifying and standardizing heart-beat cycles and segmenting the LVW, (b) introducing a novel computational biomarker—STAR-Echo—which combines spatiotemporal risk from radiomic (M_R) and deep learning (M_T) models to predict MACE prognosis in CKD patients, and (c) demonstrating the superior prognostic performance of STAR-Echo compared to M_R, M_T, as well as clinical-biomarkers (EF, BNP, and NT-proBNP) for characterizing cardiac dysfunction. STAR-Echo captured the gray level intensity distribution, perimeter and sphericity of the LVW that changes differently over time in individuals who encounter MACE outcomes. STAR-

R. Dhamdhere and G. Modanwal—These authors contributed equally to this work.

Supplementary Information The online version contains supplementary material available at https://doi.org/10.1007/978-3-031-43987-2_28.

H. Greenspan et al. (Eds.): MICCAI 2023, LNCS 14225, pp. 284–294, 2023.
https://doi.org/10.1007/978-3-031-43987-2_28

Echo achieved an AUC of $0.71[0.53-0.89]$ for MACE outcome classification and also demonstrated prognostic ability in Kaplan-Meier survival analysis on a holdout cohort ($S_v = 44$) of CKD patients ($N = 150$). It achieved superior MACE prognostication (p-value = 0.037 (log-rank test)), compared to M_R (p-value = 0.042), M_T (p-value = 0.069), clinical biomarkers—EF, BNP, and NT-proBNP (p-value >0.05).

1 Introduction

Cardiovascular disease (CVD) is the most common cause of mortality among patients with Chronic Kidney disease (CKD), with CVD accounting for 40-50% deaths in patients with acute CKD [1]. Echocardiography (Echo), a non-invasive imaging modality, provides a quick critical assessment of cardiac structure and function for cardiovascular disease diagnosis. Despite its usefulness, due to its nature, echo data is noisy and have poor resolution, which presents challenges in effectively interpreting and analyzing them. Measurements like Left ventricle (LV) volume captured by ejection fraction (EF), LV mass and LV geometry have been standard biomarkers for diagnosing and predicting severity of CVD [2–7]. With the availability of large-scale public dataset like EchoNet [7], various works have even assimilated recent deep learning advances like graphs CNNs [8] and transformers [9] for EF estimation using automated LV segmentation from echo videos. However, recent studies on CKD patients demonstrated that standard echo measurements based on static LV volume and morphology, such as EF, may have limited prognostic value beyond baseline clinical characteristics, as adverse outcomes are to the common occurrence inspite of a preserved EF [10–12]. As a result, studies have utilized machine learning to provide more detailed links to cardiac structure and function using echo data (measurements, images and videos) [10–14]. LV Wall (LVW) alterations have been reported as non-traditional biomarker of CVD due to pathophysiological changes, in CKD patients [15,16]. Abnormalities of the LVW motion are known prognostic marker for MACE prediction in CVD patients. [17–19]. Longitudinal dysfunction common in CKD patients, is reflected in LVW with change in morphology [13]. This dysfunction has been associated with CKD progression [10,12] and abnormalities are evident even in early stages of CKD [13]. Thus, an investigation of LVW morphology and longitudinal changes is warranted [10].

Radiomic based interpretable features have been used to model cardiac morphology for predicting disease outcomes [2]. Deep learning based transformer architectures [20] have recently been popular for modelling of spatiotemporal changes in LV [9]. Though they lack interpretability, they are able to extract novel features to model the data using attention [20]. Thus, in CKD patients, a combination of radiomic and transformer based spatiotemporal models could associate LVW changes over time with progression of CVD and potentially provide some insight into the factors implicated for MACE outcomes.

2 Prior Work and Novel Contributions

The relationship between Chronic Kidney disease (CKD) and Cardiovascular disease (CVD) is well established [1,21]. Echo provides a noisy yet effective modality for CVD prediction. Echo data (image, video or clinical measurements) has been extensively analyzed using machine learning and deep learning based techniques, to help in diagnosing heart conditions, predicting their severity, and identifying cardiac disease states [2]. Several studies have employed machine learning to predict diagnostic measurements and global longitudinal strain [22, 23]. In recent years, deep learning-based approaches have been successfully used to tackle echocardiographic segmentation, view classification and phase detection tasks [24,25]. With advent of EchoNet [7], a plethora of studies estimating EF and predicting heart failure have come up [8,9] while few others have used deep learning for prognostic prediction using cardiac measurements [23] and to model wall motion abnormalities [18].

Echo coupled with machine learning, has been a potent tool for analysis of CVD in patients with CKD [13]. Machine learning based analysis has revealed poor prognostic value of EF and LV based biomarkers for CVD risk assessment in CKD patients. [10,12]. Thus, techniques developed using EchoNet [7] dataset are potentially less useful for modeling CVD outcomes in CKD patients. The need for a novel approach investigating the longitudinal changes in cardiac structure and function has been recommended for analyzing CVD in patients with CKD [10,13].

In this study, for the first time, we employ echo video based spatiotemporal analysis of LVW to prognosticate CVD outcomes in kidney disease patients. Our code is available here - https://github.com/rohand24/STAR_Echo
Key contributions of our work are as follows:

* STAR-Echo, a novel biomarker that combines spatiotemporal radiomics and transformer-based models to capture morphological differences in shape and texture of LVW and their longitudinal evolution over time.
* Unique interpretable features: spatiotemporal evolution of sphericity and perimeter (shape-based) and LongRunHighGrayLevelEmphasis (texture-based), prognostic for CVD risk in CKD patients
* Demonstrated the superiority of STAR-Echo in the prognosis of CVD in CKD patients, compared to individual spatiotemporal models and clinical biomarkers.
* An end-to-end automated pipeline for echo videos that can identify heartbeat cycles, segment the LVW, and predict a prognostic risk score for CVD in CKD patients.

3 STAR-ECHO: Methodological Description

3.1 Notation

We denote a patient's echo video as a series of two-dimensional frames, represented as $V = [I_1, I_2, ..., I_N]$, where $I_1, I_2, ..., I_N$ represent the N phases (frames)

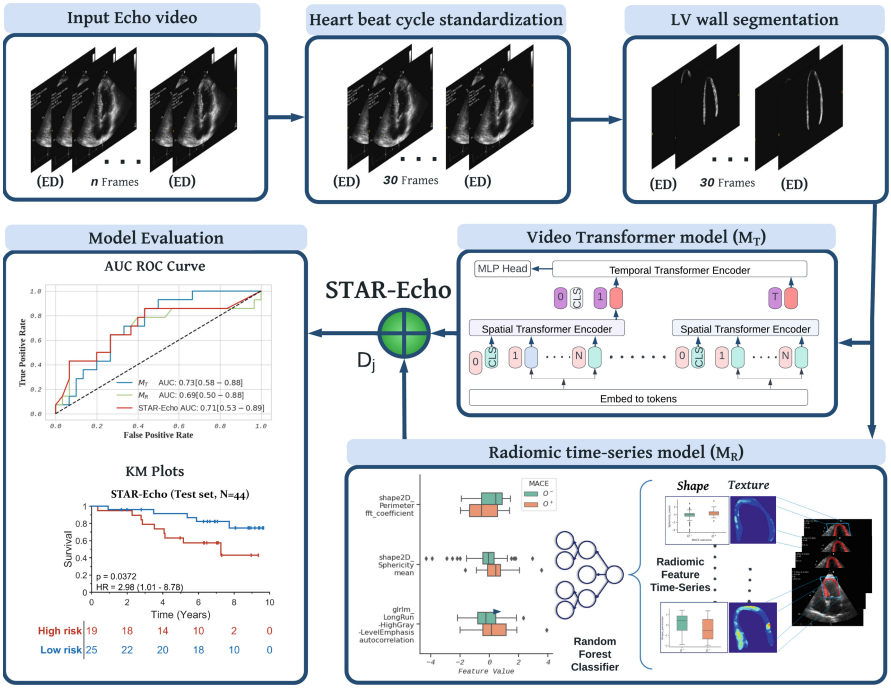

Fig. 1. Workflow of spatiotemporal analysis and STAR-Echo: STAR-Echo does fusion of complementary predictions from spatiotemporal models M_R and M_T [26]. Input echo videos are preprocessed to identify heart beat cycle between 2 end-diastolic(ED) frames. All echo videos are standardized to 30 frames. The segmented and masked LVW videos are input to the M_R and M_T pipelines.

showing the structure and function of the heart. These videos were masked with the region of interest i.e. LVW. This sequence V is preprocessed to represent one heartbeat cycle. The CVD outcomes for the patients are denoted as an event (O^+: occurrence of MACE) and non-event (O^-: no occurrence of MACE). The target outcome of a patient (O^+ or O^-) is represented by O^T.

3.2 Brief Overview

STAR-Echo comprises two spatiotemporal models (M_R, M_T). Model M_R grasps the spatiotemporal changes in the radiomic features extracted for each I_N in the echo video V for the course of one heartbeat cycle of the patient. Model M_T is a video transformer model extracting deep spatiotemporal features for echo video V of one beat cycle of the patient. M_R and M_T are separately trained and fused at Decision fusion junction D_j, to obtain STAR-Echo. The complete workflow is illustrated in Fig. 1.

3.3 Systolic Phase Extraction

The heart-beat cycle is captured using the consecutive end-diastolic phases identified by the CNN+LSTM based multi-beat echo phase detection model [25]. The heart-beat cycle frame lengths vary with individual patients. To achieve a standard frame length of 30 frames, the videos are processed with the following strategy - in videos with extra frames, random frame dropping based on normal distribution is performed, while in videos with fewer frames, a video-frame interpolation model [27] is utilized to generate frames between randomly selected adjacent frames.

3.4 Automated LVW Segmentation

Since LVW annotations were only available for the end-diastolic phase in the dataset, a weakly supervised segmentation approach is employed to obtain annotations for all phases of the echo video. Combining the available annotations with the publicly available CAMUS dataset [28], we trained a nnUNet-based U-Net [29] model for LVW segmentation. This model was then used to predict LVW for all phases, which were then checked and corrected by two expert annotators.

Masking the input echo video with LVW mask provides the echo video V, a 30-frame sequence of masked LVW image frames I_N, to be input to the spatiotemporal models M_R and M_T (Fig. 1). Additionally, each image frame I_N is center-cropped and resized to equal $k \times k$ dimensions. Thus the input to transformer model M_T is an echo video $V \epsilon \mathbb{R}^{30 \times k \times k}$.

3.5 Spatiotemporal Feature Representation

Radiomic Time-Series Model: To build this model, we employ a two-stage feature extraction process.

Radiomic Feature Extraction: In first stage, radiomic feature $R(I_N)$ is extracted on each I_N of the LVW for each phase (frame) of the echo video, V as given in (1). Radiomic features comprising of shape (10), texture (68) and first-order statistics (19) of the LVW in each phase of the echo video are extracted using pyradiomics [30] python package on the input echo phase. A total of 97 radiomic features are extracted per echo phase (frame) image I_N.

Time Series Feature Extraction: In the second stage, to model the temporal LVW motion, we consider the sequence of radiomic features from each phase of one heartbeat cycle as individual time-series. Thus, a radiomic feature time-series $t_R(V)$ is given by (2). Time-series feature T_R, as given by (3), is extracted for each radiomic feature time-series using the TSFresh library [31].

$$R(I_N) = f(I_N) \tag{1}$$

$$t_R(V) = [\, R(I_1),\, R(I_2),\, \ldots,\, R(I_N)\,] \tag{2}$$

$$T_R(V) = g(t_R(V)) \tag{3}$$

Thus, the radiomic time-series model M_R is trained on time-series features $T_R(V)$ obtained for each V of the patient to predict the outcome O^T.

Video Transformer Model: The Video Vision Transformer (ViViT) model [26] with factorised encoder is employed for this task. This architecture has two transformer encoders in series. The first encoder captures the spatial relationships between tokens from the same frame and generates a hidden representation for each frame. The second encoder captures the temporal relationships between frames, resulting in a "late fusion" of temporal and spatial information. The transformer model M_T is trained with input echo video V masked with LVW to predict the patient outcome O^T. Supplementary table S3 gives the important hyperparameters used for training the model M_T.

3.6 Model Fusion

The predictions from radiomic time-series model, M_R and video transformer model, M_T are fused at the junction D_j linear discriminant analysis (LDA) based fusion, with the output prediction probability P given by (4)

$$\log P(y = k|X_i) = \omega_k X_i + \omega_{k0} + C. \tag{4}$$

where ω_k, ω_{k0} are the learned parameters of the model and input X_i for patient i is the linear combination of the predictions of M_R and M_T given as in (5),

$$X_i = M_R(T(R(I_N))_i) + M_T(V_i) \tag{5}$$

4 Experimental Results and Discussion

4.1 Dataset Description

The dataset consisted of echo videos from patients with CKD ($N = 150$) and their composite CVD outcomes and clinical biomarker measurements for Ejection Fraction (EF), B-type natriuretic peptide (BNP) and N-terminal pro-B-type natriuretic peptide (NT-proBNP). It was stratified into 70% training ($S_t = 101$) and 30% holdout set ($S_v = 44$) The reported cardiovascular outcome, O^T, is composite of following cardiovascular events - chronic heart failure, myocardial infarction and stroke. The patients were participants of the Chronic Renal Insufficiency cohort (CRIC) [21] and their data was retrospectively made available

Table 1. Performance of M_R, M_T, STAR-Echo, clinical biomarkers in predicting O^T.

Model	Acc. (%)	AUC [95% CI]	SENS. (%)	SPEC. (%)	p-value	HR
STAR-Echo	70.45	0.71 [0.53-0.89]	64.29	73.33	0.037	2.98 [1.01-8.78]
M_R	70.45	0.69 [0.50-0.88]	64.29	73.33	0.043	3.40 [1.19-9.71]
M_T	68.18	0.73 [0.58-0.88]	68.18	35.63	0.069	2.56 [0.85-7.72]
EF(<50)	65.91	0.54 [0.36-0.72]	14.28	90.00	0.59	1.50 [0.26-8.6]
BNP(>35)	59.90	0.63 [0.44-0.81]	78.57	50.00	0.096	2.82 [0.98-8.11]
NT-proBNP(>125)	59.90	0.66 [0.47-0.84]	78.57	50.00	0.089	2.87 [1.0-8.26]

for this work. The CRIC study [21] is on individuals with mild to moderate CKD, not on dialysis. Diabetes is the main reported comorbidity for the study. The study followed the patients for CVD outcomes. Additional details along with inclusion-exclusion criteria of the dataset are included in the supplementary materials. In the dataset, a total of 46 patients experienced the composite event outcome. The dataset also included survival time information about the patients. The median survival time for patients, O^T was 6.5 years (median O^- = 6.7 years, median O^+ = 3.5 years).

4.2 Statistical and Survival Analysis

Statistical Feature Selection – Extracted times-series features (T_R) are normalized and multicollinear features are excluded. Analysis of Variance (ANOVA) based stable feature selection ($p < 0.002$) and Brouta [32] based all-relevant feature selection ($\alpha = 0.05, threshold = 0.98$) is applied sequentially. A Random forest classifier was trained on the training set using 5-fold cross-validation across 100 iterations, and the best model was selected based on AUC. The selected model was applied to the holdout set, and performance metrics were reported.

Survival Analysis – KM plots with log-rank test analyzed the prognostic ability of models. The curves showed survival time (in years) on the horizontal axis and probability of survival on the vertical axis, with each point representing survival probability of patients. Hazard ratios and p-values were reported for significance between low-risk and high-risk cohorts.

4.3 Evaluating Ability of STAR-ECHO to MACE Prognosis

MACE prognosis is a necessary task in CKD patients management due to high CVD events in CKD patients [33]. Figure 2 shows the KM curves for each indi-

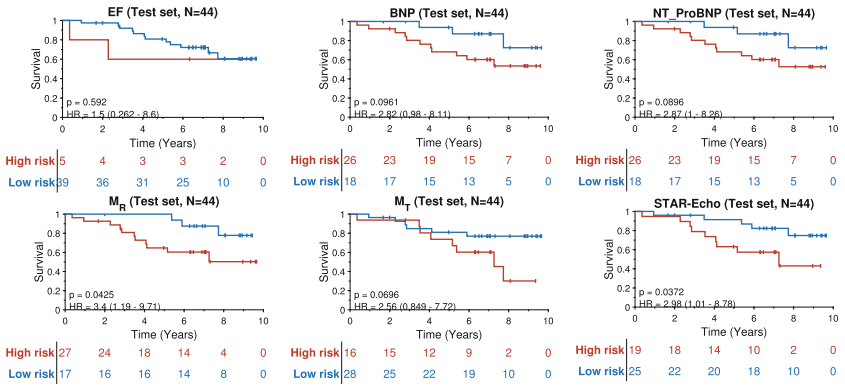

Fig. 2. Risk severity analysis using KM curves - Risk stratification using log-rank test shows significant separation only for M_R and *STAR-Echo* (bottom row). $STAR - Echo$ model demonstrates improved significance (p = 0.037) and high hazard ratio (HR = 2.98[1.01 - 8.78]) indicative of prognosis for CVD risk prediction in CKD.

vidual models on the holdout set ($S_v = 44$). Significant separation($p < 0.05$) is observed for models M_R and STAR-Echo. None of the clinical biomarker models have significant separation. Thus, the models trained on EchoNet [7], relying on EF, would not provide a prognostic prediction. Thus, the radiomics features aid in prognosis of MACE risk in CKD patients. The combination model, STAR-Echo, outperforms all the individual models with better risk stratification ($p = 0.037$ and $HR = 2.98$) than individual spatiotemporal models($M_R : p = 0.042; M_T : p = 0.069$) and shows high accuracy in prediction compared to M_R and M_T models. Thus we are able to showcase that saptiotemporal changes in the shape and texture of LVW are prognostic markers for MACE outcomes in CKD patients.

Accuracy, area under the ROC curve (AUC), sensitivity, specificity were the prediction metrics and p-value and hazard ratios (HR) were the prognosis metrics observed (Table 1) for all the models, with the model STAR-Echo achieving the highest Accuracy of 70.45% with a significant p-value(= 0.0372) and high HR(= 2.98). No statistically significant difference is observed in AUC performances of the different spatiotemporal models, indicating that the video transformer and the radiomic time-series models are capturing similar spatiotemporal changes in the shape and intensities of the LVW. The individual clinical biomarker based models performed poorly consistent with observations in CKD patients [10,12]. Thus EchoNet [7] based models would perform poorly in predicting the MACE outcomes as well.

The top radiomic features (Fig. 3-A) include longitudinal changes in perimeter and sphericity of the LVW shape along with intensity changes in the LVW texture. The texture feature changes in systolic function and the shape differences over different frames can be observed in Fig. 3-B. Changes in the LVW shape can indicate left ventricular hypertrophy (LVH), a common complication of CKD linked to a higher risk of cardiovascular events. LVH can stem from

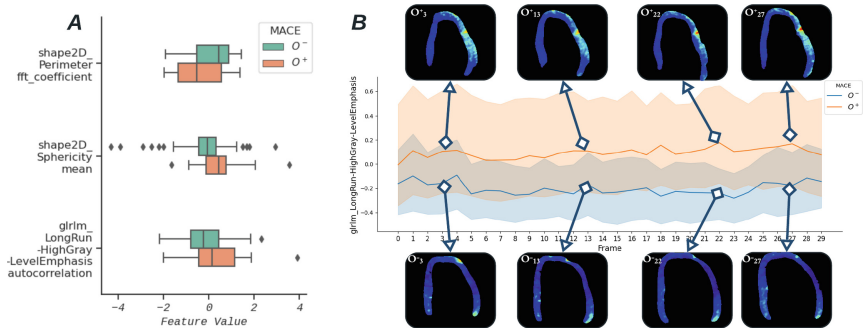

Fig. 3. (A) Top features with significant differences ($p < 0.05$) between MACE outcomes (O^- and O^+). (B) The mean feature value difference over time for selected texture feature, between O^- and O^+. The $3^{rd}, 13^{th}, 22^{th}, 27^{th}$ frames are shown for example O^- and O^+ cases. Clear differences in texture and shape are observed between O^- and O^+, evolving over time.

various factors that modify the ventricle's structure and geometry [15]. Texture changes in LV may also reflect alterations in collagen content or fibrosis which increase the risk of adverse events associated with cardiac remodeling [15].

5 Conclusion

In this study, we introduced STAR-Echo, a novel biomarker combining radiomics and video transformer-based descriptors to evaluate spatiotemporal changes in LVW morphology. STAR-Echo identifies novel features based on longitudinal changes in LVW shape (perimeter and sphericity) and texture (intensity variations) over a heartbeat cycle, similar to recent clinical pathophysiological findings of CVD in CKD [15]. Results show that STAR-Echo significantly improves CVD prognosis in CKD patients ($AUC = 0.71, p = 0.0372, HR = 2.98$) compared to clinical biomarkers, potentially outperforming EchoNet [7] based LV volume-based approaches. Future research will validate STAR-Echo in a larger patient population and incorporate clinical data for improved management of CVD and CKD.

Acknowledgement. Research reported in this publication was supported by the National Cancer Institute under award numbers R01CA268287A1, U01 CA269181, R01CA26820701A1, R01CA249992-01A1, R0CA202752-01A1, R01 CA208236-01A1, R01CA216579-01A1, R01CA220581-01A1, R01CA257612-01A1, 1U01CA239055-01, 1U01CA248226-01, 1U54CA254566-01, National Heart, Lung and Blood Institute 1R01HL15127701A1, R01HL15807101A1, National Institute of Biomedical Imaging and Bioengineering 1R43EB028736-01, VA Merit Review Award IBX004121A from the United States Department of Veterans Affairs Biomedical Laboratory Research and Development Service the Office of the Assistant Secretary of Defense for Health Affairs, through the Breast Cancer Research Program (W81XWH-19-1-0668), the Prostate Cancer Research Program (W81XWH-20-1-0851), the Lung Cancer Research Program (W81XWH-18-1-0440, W81XWH-20-1-0595), the Peer Reviewed Cancer Research Program (W81XWH-18-1-0404, W81XWH-21-1-0345, W81XWH-21-1-0160), the Kidney Precision Medicine Project (KPMP) Glue Grant and sponsored research agreements from Bristol Myers-Squibb, Boehringer-Ingelheim, Eli-Lilly and Astra-zeneca. The content is solely the responsibility of the authors and does not necessarily represent the official views of the National Institutes of Health, the U.S. Department of Veterans Affairs, the Department of Defense, or the United States Government.

References

1. Marx, N., Floege, J.: Dapagliflozin, advanced chronic kidney disease, and mortality: new insights from the DAPA-CKD trial. Eur. Heart J. **42**(13), 1228–1230 (2021)
2. Barry, T., Farina, J.M., et al.: The role of artificial intelligence in echocardiography. J. Imaging **9**, 50 (2023)
3. Zhang, J., Gajjala, S., et al.: Fully automated echocardiogram interpretation in clinical practice. Circulation **138**, 1623–1635 (2018)
4. Yang, F., Chen, X., et al.: Automated analysis of doppler echocardiographic videos as a screening tool for valvular heart diseases. JACC Cardiovasc. Imaging **15**, 551–563 (2022)

5. Hwang, I.-C., Choi, D., et al.: Differential diagnosis of common etiologies of left ventricular hypertrophy using a hybrid CNN-LSTM model. Sci. Rep. **12**, 20998 (2022)
6. Liu, B., Chang, H., et al.: A deep learning framework assisted echocardiography with diagnosis, lesion localization, phenogrouping heterogeneous disease, and anomaly detection. Sci. Rep. **13**, 3 (2023)
7. Ouyang, D., He, B., et al.: Video-based AI for beat-to-beat assessment of cardiac function. Nature **580**, 252–256 (2020)
8. Mokhtari, M., Tsang, T., et al.: EchoGNN: explainable ejection fraction estimation with graph neural networks. In: Wang, L., Dou, Q., Fletcher, P.T., Speidel, S., Li, S. (eds.) MICCAI 2022. LNCS, vol. 13434, pp. 360–369. Springer, Cham (2022). https://doi.org/10.1007/978-3-031-16440-8_35
9. Muhtaseb, R., Yaqub, M.: EchoCoTr: estimation of the left ventricular ejection fraction from spatiotemporal echocardiography. In: Wang, L., Dou, Q., Fletcher, P.T., Speidel, S., Li, S. (eds.) MICCAI 2022. LNCS, vol. 13434, pp. 370–379. Springer, Cham (2022). https://doi.org/10.1007/978-3-031-16440-8_36
10. Fitzpatrick, J.K., Ambrosy, A.P., et al.: Prognostic value of echocardiography for heart failure and death in adults with chronic kidney disease. Am. Heart J. **248**, 84–96 (2022)
11. Mark, P.B., Mangion, K., et al.: Left ventricular dysfunction with preserved ejection fraction: the most common left ventricular disorder in chronic kidney disease patients. Clin. Kidney J. **15**, 2186–2199 (2022)
12. Zelnick, L.R., Shlipak, M.G., et al.: Prediction of incident heart failure in CKD: the CRIC study. Kidney Int. Rep. **7**, 708–719 (2022)
13. Dohi, K.: Echocardiographic assessment of cardiac structure and function in chronic renal disease. J. Echocardiogr. **17**, 115–122 (2019)
14. Christensen, J., Landler, N.E., et al.: Left ventricular structure and function in patients with chronic kidney disease assessed by 3D echocardiography: the CPH-CKD ECHO study. Int. J. Cardiovasc. Imaging **38**, 1233–1244 (2022)
15. Jankowski, J., Floege, J., et al.: Cardiovascular disease in chronic kidney disease. Circulation **143**, 1157–1172 (2021)
16. Bongartz, L.G., Braam, B., et al.: Target organ cross talk in cardiorenal syndrome: animal models. Am. J. Physiol. Renal Physiol. **303**, F1253–F1263 (2012)
17. Kamran, S., Akhtar, N., et al.: Association of major adverse cardiovascular events in patients with stroke and cardiac wall motion abnormalities. J. Am. Heart Assoc. **10**, e020888 (2021)
18. Huang, M.-S., Wang, C.-S., et al.: Automated recognition of regional wall motion abnormalities through deep neural network interpretation of transthoracic echocardiography. Circulation **142**, 1510–1520 (2020)
19. Elhendy, A., Mahoney, D.W., et al.: Prognostic significance of the location of wall motion abnormalities during exercise echocardiography. J. Am. Coll. Cardiol. **40**, 1623–1629 (2002)
20. Vaswani, A., Shazeer, N., et al.: Attention is all you need. In: Advances in Neural Information Processing Systems, vol. 30, Curran Associates Inc. (2017)
21. Feldman, H., Dember, L.: Chronic renal insufficiency cohort study (2022). Artwork Size: 263268080 MB Pages: 263268080 MB Version Number: V11 Type: dataset
22. Salte, I.M., Østvik, A., et al.: Artificial intelligence for automatic measurement of left ventricular strain in echocardiography. JACC Cardiovasc. Imaging **14**, 1918–1928 (2021)

23. Pandey, A., Kagiyama, N., et al.: Deep-learning models for the echocardiographic assessment of diastolic dysfunction. JACC Cardiovasc. Imaging **14**, 1887–1900 (2021)
24. Zamzmi, G., Rajaraman, S., et al.: Real-time echocardiography image analysis and quantification of cardiac indices. Med. Image Anal. **80**, 102438 (2022)
25. Lane, E.S., Azarmehr, N., et al.: Multibeat echocardiographic phase detection using deep neural networks. Comput. Biol. Med. **133**, 104373 (2021)
26. Arnab, A., Dehghani, M., et al.: ViViT: a video vision transformer. In: 2021 IEEE/CVF International Conference on Computer Vision (ICCV), Montreal, QC, Canada, pp. 6816–6826. IEEE (2021)
27. Cheng, X., Chen, Z.: Multiple video frame interpolation via enhanced deformable separable convolution. IEEE Trans. Pattern Anal. Mach. Intell. **44**, 7029–7045 (2022)
28. Leclerc, S., Smistad, E., et al.: Deep learning for segmentation using an open large-scale dataset in 2D echocardiography. IEEE Trans. Med. Imaging **38**, 2198–2210 (2019)
29. Isensee, F., Jaeger, P.F., et al.: nnU-Net: a self-configuring method for deep learning-based biomedical image segmentation. Nat. Methods **18**, 203–211 (2021)
30. van Griethuysen, J.J., Fedorov, A., et al.: Computational radiomics system to decode the radiographic phenotype. Can. Res. **77**, e104–e107 (2017)
31. Christ, M., Braun, N., et al.: Time series feature extraction on basis of scalable hypothesis tests (tsfresh - a python package). Neurocomputing **307**, 72–77 (2018)
32. Kursa, M.B., Rudnicki, W.R.: Feature selection with the Boruta package. J. Stat. Softw. **36**, 1–13 (2010)
33. Jain, N., McAdams, M., et al.: Screening for cardiovascular disease in CKD: PRO. Kidney360 **3**, 1831 (2022)